AIChE

Kinetics and Mechanism of Solid Reactions in a Micro Fluidized Bed Reactor

Jian Yu, Junrong Yue, Zhouen Liu, Li Dong, and Guangwen Xu
State Key Laboratory of Multi-phase Complex System, Institute of Process Engineering, Chinese Academy of Sciences, Beijing 100190, China

Jianhong Zhu and Zhengkang Duan
Chemical Engineering Institute of Xiangtan University in Hunan Province, Xiangtan 411105, China

Lixin Sun
Beijing Henven Scientific Instrument Co. Ltd, Beijing 101400, China

DOI 10.1002/aic.12205
Published online March 19, 2010 in Wiley Online Library (wileyonlinelibrary.com).

A novel gas–solid Micro Fluidized Bed Reaction Analyzer (MFBRA) was developed to deduce reaction rates and kinetic parameters through measuring time-dependent composition changes of evolved gases from the reactions. Application of the MFBRA to the decomposition of $CaCO_3$ powder resulted in an apparent activation energy of 142.73 kJ/mol and a pre-exponential factor of 399,777 s^{-1}. This apparent activation energy was much lower than the thermogravimetry-measured value of 184.31 kJ/mol, demonstrating a quicker reaction in the MFBRA. This was further verified by CuO reduction in CO, as accelerated by the fast diffusion and high heating rate in the MFBRA. Measurement of pyrolysis of coal and biomass in MFBRA found that the reaction process was completed in about 10 s, a time much shorter than the literature-reported values in larger fluidized bed reactors. By monitoring the release of gas species from reactions at different temperatures, the MFBRA also allowed deeper insight into the mechanism of pyrolysis reactions. © 2010 American Institute of Chemical Engineers *AIChE J,* 56: 2905–2912, 2010
Keywords: micro fluidized bed, kinetics, gas–solid reaction, pyrolysis

Introduction

The common experimental method of studying the kinetics of thermally activated reactions of solids is thermogravimetry (TG), differential thermal analysis (DTA), and differential scanning calorimetry (DSC). These techniques are widely applied to many types of reactions, such as thermal decomposition of materials,[1–3] crystallization of polymers,[4] regeneration of deactivated catalyst,[5] and reduction or oxidation of iron ore,[6,7] although the methods are inherently unable to unravel the kinetics at a given temperature. In fact, the TG-based instruments measure the mass loss or thermal variation of a sample with time and temperature during a specified heating program. For this, the sample has to be set into a reaction cell before the heating process is started. Consequently, the reactions occurring in TG instruments suffer seriously from external diffusion. Especially, some energy materials such as coal and biomass are unsuitable for testing with TG due to the quick change of their compositions with increasing temperature.

The micro fluidized bed reaction analyzer (MFBRA) was developed to enable (1) on-line pulse feeding and rapid heating of particle reactant, (2) effective suppression of the interfacial diffusion limitations in the reactor, and (3)

Correspondence concerning this article should be addressed to G. Xu at gwxu@home.ipe.ac.cn; or J. Yu, at E-mail: yujian@home.ipe.ac.cn.

minimization of the intra-particle diffusion through utilization of fine solid reactants. Hence, the MFBRA provides a measurement of reaction rates at arbitrary temperatures, which is impossible for the thermogravimetric analyzers that measure only the mass loss and neglect the variation in the nature of sample during temperature rises. Furthermore, by combining with a mass spectrometer (MS) and an electrochemical sensor to analyze the gaseous products, the MFBRA can provide information on the mechanism of the reaction. Consequently, the MFBRA would be particularly suitable to study the kinetics of fast gas–solid reactions, such as pyrolysis of coal and regeneration of FCC catalyst.

This study utilizes MFBRA to analyze $CaCO_3$ decomposition and calculate the kinetic parameters of the reaction. To compare the capabilities of the MFBRA and TG, the reduction of CuO in CO was carried out with both the MFBRA and TG at the same temperature. Pyrolysis of biomass and coal in Ar atmosphere were further performed in the MFBRA connected to a mass spectrometer to demonstrate the applicability of the newly developed reaction analysis tool for quick reactions. This provided as well a further study on the sequence of evolvement and yield variation of key gas components in raising temperature.

MFBRA: Design and Experiment

Figure 1a is a schematic diagram of the MFBRA, which consists of a solid sample jet-transfer device, a fluidized bed reactor of 20 mm in diameter filled with 0.25 mm diameter quarts sands, and a gas cleaning and analysis system. The solid sample jet-transfer device, which injects a sample into the micro fluidized bed reactor in less than 0.1 s with a compressed gas stream at 0.2 MPa through a sample tube of 3 mm in diameter, was driven by controlling an electromagnetic valve that releases about 10 NML per single pulse. The micro fluidized bed reactor consists of two stages, the lower stage to receive the test sample at selected temperatures and the top stage to catch the fine sample particles escaping from the bottom stage. Our previous study[8] revealed that bubbling/turbulent fluidization is likely to prevail in the micro fluidized bed reactor. The gas cleaning and analysis system of the MFBRA consist of a gas condenser, a filter, and an on-line mass spectrometer (MS) or a few gas detection sensors. The gas condensation and filter was designed to avoid the leakage of large molecule organics (i.e., tar in the pyrolysis gas of coal or biomass) into the gas detector. When MS was adopted, a heated capillary tube at temperatures of about 350°C was used to collect the filter and the MS. The furnace temperature, carrier gas flow rate, sample jet-valve, and effluence gas detectors were all connected to a computer to monitor the variations of parameters under the control of a self-programed software. The software includes the codes for a few commonly used kinetic models like *n*-diffusion model, shrinking-core model, and power-law model to calculate the kinetic parameters from the measured data of gas flow rate, temperature, and gas composition. The temperature in the reactor could reach 950°C with fluctuations of about ±10°C. Figure 1b presents a photograph of the MFBRA system, showing that the analyzer was well integrated and highly compact. Experimental results showed that

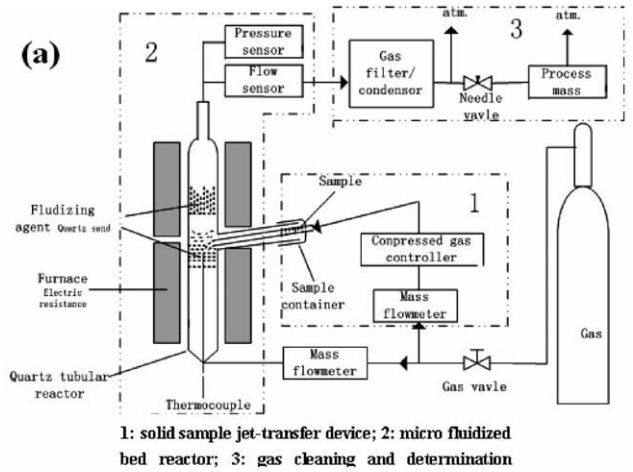

1: solid sample jet-transfer device; 2: micro fluidized bed reactor; 3: gas cleaning and determination

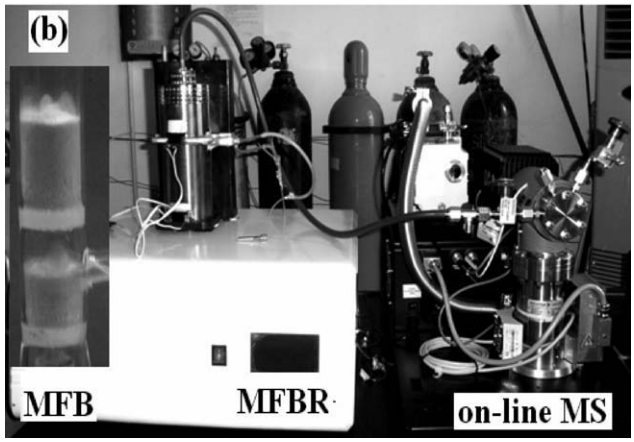

Figure 1. Schematic diagram (a) and photograph (b) of micro fluidized bed reaction analyzer system.

the repeatability error of the analyzer was within ±3.0% and the time delay of analyzing response was less than 3 s.

The experiment with MFBRA was performed generally according to the following procedure. Three grams of fluidizing medium particles (quartz sand here) was put into each layer of the reactor. Under controlled fluidizing gas stream of 200 ml/min (room conditions), the furnace heated the fluidized sand particles to a selected temperature below 950°C. A solid sample of 10–50 mg and 45–75 μm in diameter was in turn injected into the inside of the hot fluidized quartz sand particles to initiate the reaction. For the reduction of CuO reported herein, a slightly different experimental procedure was adopted. After the sample was injected into the reactor, about 1 min of stabilization time was applied to allow the sample be heated to the bed temperature. Then, the reduction of CuO was started by switching the fluidizing gas from Ar to CO. This operation was suggested to ensure the reaction conditions similar to that in the TG test where the reaction was also initiated by gas switching at a preset temperature. For all TG tests reported in this article, a gas flow rate of 50 ml/min was adopted.

The tested $CaCO_3$ and CuO materials were with analytical purity and purchased from China National Medicines Corporation. The pyrolysis experiments were performed with respect to a kind of beer lees and a Xinjiang brown coal

Table 1. Properties of Biomass and Coal

	Beer Lees	Brown Coal
Proximate analysis (a.d.) (% wt/wt)		
Ash (a.d.)	3.93	9.42
Volatile matter (a.d.)	79.9	30.02
Fixed carbon (a.d.)	16.17	60.56
Ultimate analysis (d.a.f.) (% wt/wt)		
C	48.74	71.05
H	6.73	3.87
N	4.58	1.02
S+O	38.95	24.06
Atomic H/C	1.66	0.65

a.d. and d.a.f. denote air dry and dry ash free, respectively.

characterized in Table 1. Both the fuels were predried at 110°C for 10 h.

Results and Discussion

Thermal decomposition of $CaCO_3$ using TG

The decomposition kinetics of $CaCO_3$ in the TG instrument was studied in Ar atmosphere with different heating rate. The apparent activation energy under different conversions α was derived using the Flynn-Wall-Ozawa method[9] that can be mathematically expressed via the following equations:

$$d\alpha/dt = k(T)F(\alpha) = A\exp\left(\frac{-E}{RT}\right)F(\alpha), \tag{1}$$

$$\int_0^{\alpha}\frac{d\alpha}{F(\alpha)} = \int_0^{t} A\exp\left(\frac{-E}{RT}\right)dt, \tag{2}$$

$$T/t = \beta,\ u = \frac{E}{RT},\ G(\alpha) = \int_0^{\alpha}[F(\alpha)]^{-1}d\alpha, \tag{3}$$

$$G(\alpha) = \frac{A}{\beta}\int_0^{T}\exp\left(\frac{-E}{RT}\right)dT = \frac{AE}{\beta R}\int_{\infty}^{u}\frac{-e^u}{u^2}du = \frac{AE}{\beta R}\bullet P(u), \tag{4}$$

$$\lg P(u) = -2.315 - 0.4567\frac{E}{RT}, \tag{5}$$

$$\lg\beta = \ln\frac{AE}{RG(\alpha)} - 2.315 - 0.4567\frac{E}{RT}, \tag{6}$$

$$\alpha = \frac{m_0 - m_t}{m_0 - m_e}, \tag{7}$$

where A is the frequency factor, E is the apparent activation energy, R is the gas constant, β is the heating rate, $G(\alpha)$ represents the integration of $F(\alpha)$ over the conversion range of 0–α, $F(\alpha)$ is a function of α, α is the reaction conversion, and m_0, m_t, and m_e represent the $CaCO_3$ mass at time 0, time t, and the test end, respectively.

The Flynn-Wall-Ozawa method is widely adopted to analyze the nonisotherm reaction process occurring in TG. In this case, the realized different conversions correspond to different reaction temperatures. Thus, only for a given conversion, both $F(\alpha)$ and $G(\alpha)$ can be constants. Equation 6, derived from Eq. 2 via mathematical transformation, is the so-called F-W-O equation, which defines an activation energy E for each given conversion α. The activation energy at $\alpha = 0$ can then be determined through extrapolating the correlation curve of E vs. α and typified to represent the activation energy for the tested reaction.

Figure 2 shows the conversion of $CaCO_3$ vs. temperature at different heating rates. The temperature of initial decomposition of $CaCO_3$ decreased with lowering the heating rate. This suggests that elevating the heating rate increased the gradients of temperature as well as the heat transfer between the sample and the temperature measuring point. At a higher heating rate, a greater temperature lag of the sample from the measured value was therefore responsible for the higher explicit decomposition temperature.

The Flynn-Wall-Ozawa equation implies that the term $\lg\beta$ is subjected to a linear correlation with $1/T$ at a constant α. This allows the apparent activation energy E to be determined against different α based on the conversion data in Figure 2. The results demonstrated that E varied with the conversion α, as is shown in Figure 3. This reveals in fact a feature of the nonisothermal reactions in TG and is possibly related to the differences in diffusion, reactant, and temperature at different α. Polynomial fitting of the apparent activation energy E and the conversion α resulted in the equation and the curve shown in Figure 3 (correlation coefficient r being 0.99). Extrapolating the curve to $\alpha = 0$ resulted in $E_\alpha = 0$ of 184.31 kJ/mol. According to the Flynn-Wall-Ozawa approach, this $E_\alpha = 0$ represents the apparent activation energy to initiate the $CaCO_3$ decomposition to form the new product phase of CaO.

Thermal decomposition of $CaCO_3$ in a MFBRA

Decomposition of $CaCO_3$ was carried out in a MFBRA at 700–900°C. For fluidized bed reactor, the diffusional and nonisothermal effects can be negligible in this temperature range so that the decomposition reaction in the MFBRA can be considered to be under isothermal conditions.

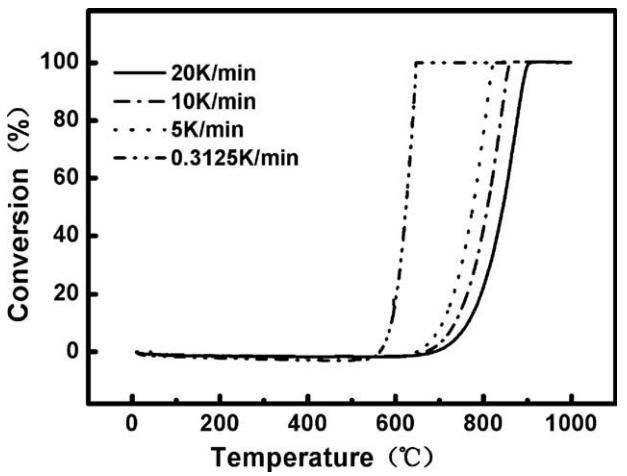

Figure 2. Relationship between conversion and temperature of $CaCO_3$ decomposition in TG at different heating rates.

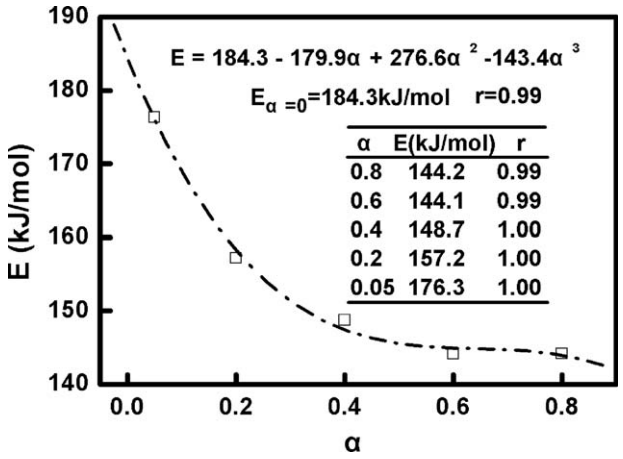

Figure 3. Correlation of activation energy *E* and conversion α derived from the data in Figure 2.

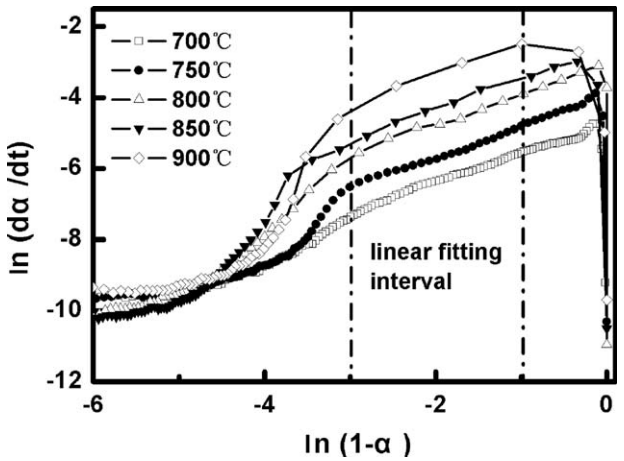

Figure 5. Correlation of ln($d\alpha/dt$) and ln(1−α) for $CaCO_3$ decomposition in MFBRA.

Conversion of $CaCO_3$ (α) was calculated by:

$$\alpha(\%) = \frac{100\sum FC_{CO_2}}{22.4 m_{CaCO_3}} \times 100\%, \quad (8)$$

where m_{CaCO3} denotes the mass of $CaCO_3$ sample, F refers to the flow rate of effluent gas, and C_{CO2} is the CO_2 molar concentration in the gas.

The kinetic parameters of $CaCO_3$ decomposition reaction were generally calculated using the shrinking-core model.[10] This model suggests that the reaction rate can be related to the unreacted surface area or remaining amount of reactant. The model can be expressed with Eq. 9, where n is the reaction order and $k(T)$ is the reaction rate constant defined by the Arrhenius Equation [Eq. 10]:

$$d\alpha/dt = k(T) \times (1-\alpha)^n, \quad (9)$$

$$\ln[k(T)] = \ln(A) - \frac{E}{RT}. \quad (10)$$

.

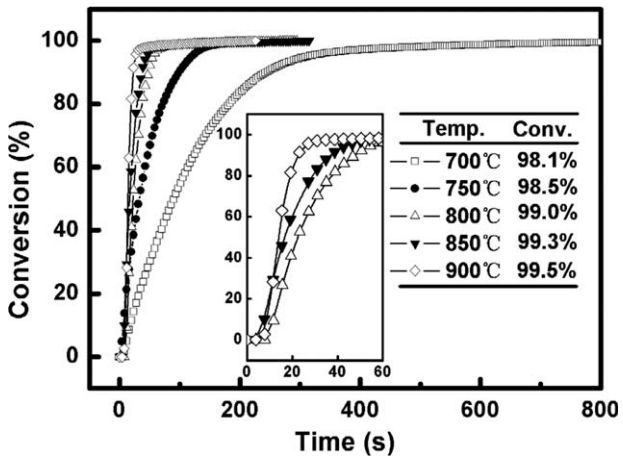

Figure 4. Conversion vs. reaction time of $CaCO_3$ decomposition in MFBRA at different temperatures.

Figure 4 shows the conversion of $CaCO_3$ vs. reaction time at different temperatures realized in MFBRA. Surely, increasing temperature increased the reaction rate, and Figure 4 shows that the decomposition completion time was short as 10 s at 900°C (see the inset plot), which was much quicker than that in Figure 2 for TG. The realized decomposition conversion was over 98% at all the tested temperatures, suggesting that the MFBRA has good reliability and repeatability.

Figure 5 converts the data of Figure 4 into the correlation of ln($d\alpha/dt$) and ln(1−α). The entire curve for a given temperature can be divided into three parts denoting three reaction stages. The first part (right side) belongs to the sample heating stage. Thus, the higher the reaction temperature, the wider this stage was. The reaction rate $d\alpha/dt$ at the end of this stage was also higher at higher temperature, complying with the nature that the reaction in this stage occurred mainly on the sample surfaces.

As a layer of CaO was formed around the $CaCO_3$ particle, the decomposition shifted into the second stage, the major period to implement the decomposition. In this stage, the intra-particle diffusion of CO_2 became gradually important and even turned to be the rate-controlling step of the decomposition reaction. This is why in Figure 5 ln($d\alpha/dt$) reduced linearly with increasing ln(1−α) calculated from the remaining amount of $CaCO_3$ reactant (note: reaction temperature being in a stable constant). Once the intra-particle CO_2 diffusion completely controlled the reaction and the reactant was close to complete depletion, the reaction rate began to decrease quickly with the progress of reaction. This refers to the start of the third reaction stage.

The data of the second reaction stage shown in Figure 5 were re-plotted in Figure 6 to define the reaction order n and rate constant $k(T)$ for different temperatures. At all temperatures, the data are subjected to a good linear fitting of ln($d\alpha/dt$) with ln(1−α). The data tabulated in Figure 7 shows that a linear correlation coefficient r reached 0.99 for all the curves.

The derived parameters n and $k(T)$ are correlated in Figure 7. The obtained reaction orders for all tested temperatures are about 0.86 and shared little difference, suggesting a

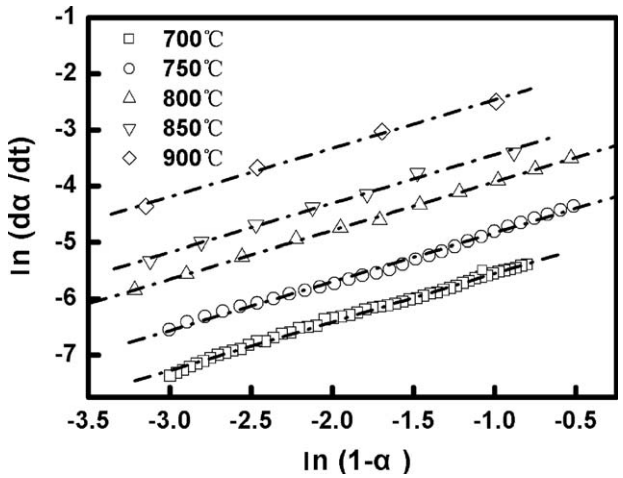

Figure 6. Linear fitting of ln($d\alpha/dt$) and ln($1-\alpha$) for $CaCO_3$ decomposition in MFBRA.

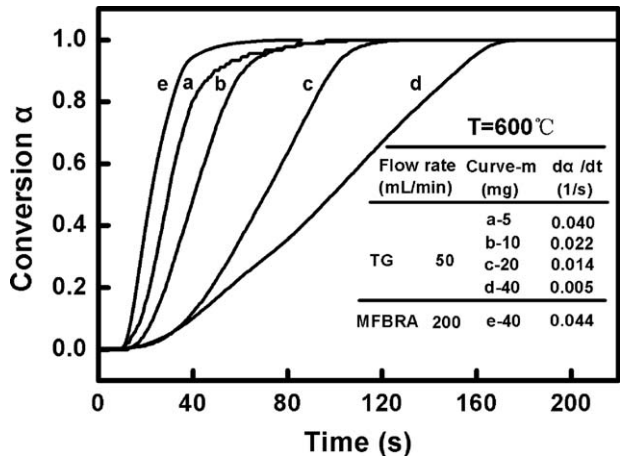

Figure 8. Reduction rate of CuO in CO and conversion of CuO vs. reaction time measured in both TG and MFBRA.

good measurement repeatability of the MFBRA. This demonstrates also that the kinetic model shown with Eq. 4 describes well the $CaCO_3$ decomposition reaction. The Arrhenius correlation for $k(T)$ in Figure 7 defines the frequency factor A of 399,777 s^{-1} and the apparent activation energy E of 142.73 kJ/mol. This apparent activation energy value fell into the range of 120–280 kJ/mol reported in the literature[11] and was obviously lower than the above-acquired TG result of 184.31 kJ/mol. This shows that the reaction rate in the MFBRA was much faster than in TG, verifying that the MFBRA allowed good mass and heat transfer as well as good measurement of the reaction rate and kinetics compared to TG.

Reduction of CuO with CO

Reaction of CuO in CO was tested with TG and the MFBRA to compare their realized reaction rates at a given reaction temperature. The MFBRA measured the formed CO_2 in its effluent gas, whereas TG monitored the sample weight change. Figure 8 shows the realized conversion as a function of reaction time. The TG tests were carried out for different sample amounts (5–40 mg), demonstrating that increasing the sample mass decreased the reaction rate (see the slope of each curve or the rate data of 0.04–0.005 s^{-1}). This reveals that the reaction with TG suffered greatly from the diffusion of CO into the CuO sample held in the TG cell. The test in the MFBRA used 40 mg of sample, the largest mass amount used in the TG tests, but the realized reaction rate (0.044 s^{-1}) was even higher than that from testing 5 mg sample in TG (i.e., curve e against curve a). This suggests that the influence of external diffusion was much smaller in the MFBRA than in TG, as a result of using a fluidized bed reactor in the MFBRA. This corroborates the advantage of the MFBRA in suppressing the external diffusion, a significant limitation for TG.

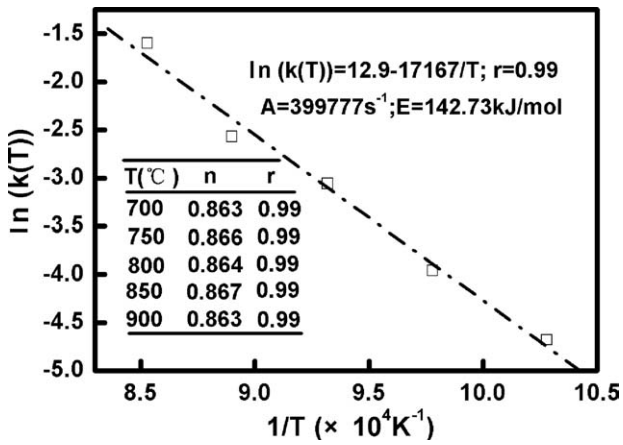

Figure 7. Reaction order at different temperatures and linear fitting of ln[$k(T)$] and $1/T$ for $CaCO_3$ decomposition in MFBRA.

Pyrolysis of biomass in MFBRA

Pyrolysis of biomass and coal is a high-speed reaction, which can hardly be correctly analyzed with TG, especially for measuring the reaction completion time and characterizing the product gas release sequence. Therefore, scholars designed various different reactors, including fluidized beds, to measure pyrolysis reactions. The adopted fluidized beds have usually diameters of tens of millimeters, causing serious effects of gas mixing and diffusion. Using micro fluidized bed may avoid these problems. Pyrolysis of biomass and coal were thus measured in the MFBRA to demonstrate its capability in this aspect.

Figure 9 shows the evolved H_2, CO, CO_2, and CH_4 in pyrolysis of beer lees in the MFBRA at 800°C. Overall, one can see that the pyrolysis finished in about 10 s, which is much shorter than the time (45 s) measured by Xu et al.[12] at the same temperature but in an 80 mm (i.d.) fluidized bed. The figure demonstrates that different gas species have different times to start and end the gas release process. The first released gas is CO_2, and in succession are H_2, CO, and CH_4, whereas the ending of gas release was subjected to an order of CO_2, CH_4, CO, and H_2. The time span of gas release appeared longest for H_2, shortest for CO_2, and equivalent for CH_4 and CO. These results indicate that, in pyrolysis, the

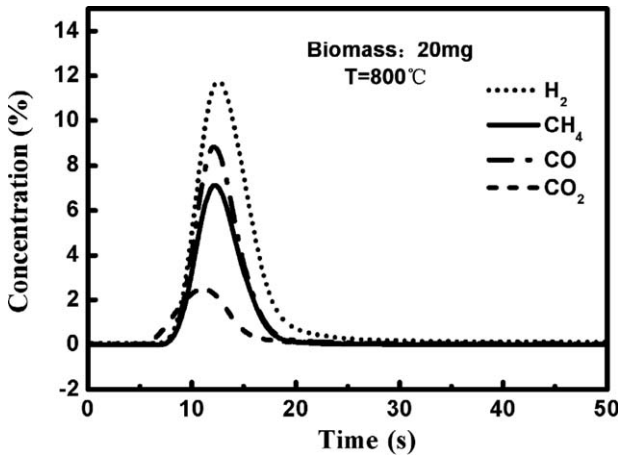

Figure 9. Evolved gases and release sequence of biomass pyrolysis vs. reaction time.

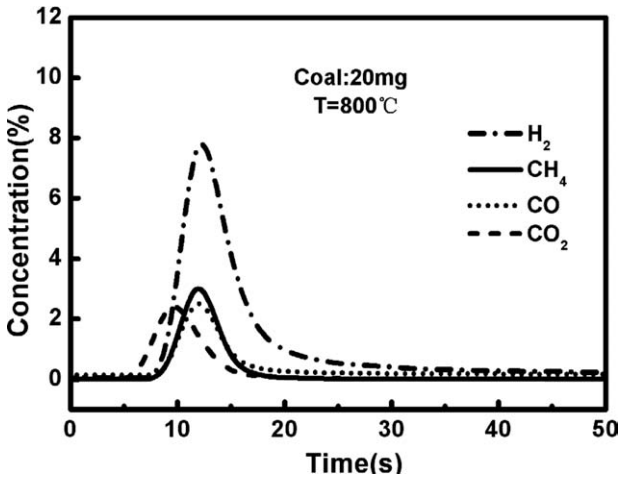

Figure 11. Evolved gases and release sequence of coal pyrolysis vs. reaction time.

gases CO_2, CH_4, CO, and H_2 are produced via different chemical routes and mechanics, such as the decomposition of different primary or secondary functional groups at different temperatures. For example, the earliest production of CO_2 should be related to the decomposition of carboxyl group which occurs likely at low temperatures.

Measuring pyrolysis of beer lees at a few other temperatures demonstrated the same gas release characteristics as depicted above. Figure 10 compares the total volumes of H_2, CO, CO_2, and CH_4 produced in pyrolysis at different temperatures. Raising the temperature from 400 to 900°C resulted in gradually larger increases in H_2 production and the generated H_2 reached 0.42 Nm^3/kg d.a.f. biomass at 900°C. Increases in the produced gas volume with raising temperature occurred at temperatures of up to 600°C for CO and up to 700°C for CH_4, respectively. Then, the CO and CH_4 productions both decreased with elevating temperature, especially for CH_4 which decreased quickly to about 0.07 Nm^3/kg d.a.f. fuel at 900°C. The formed CO_2 only slightly varied at the tested temperatures and remained as a constant at 500–800°C (0.08 Nm^3/kg d.a.f. fuel).

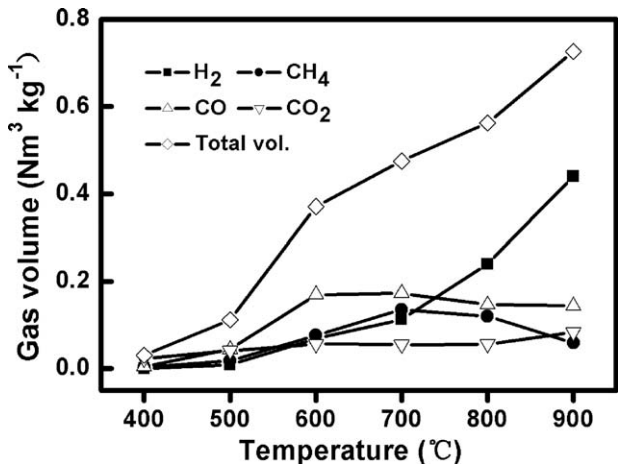

Figure 10. Permanent gas volume (Nm^3/kg a.d. biomass) as a function of reaction temperature for biomass pyrolysis.

The volume of mixed pyrolysis gas exhibited obvious increase with increasing temperature, say, from 0.03 to 0.72 Nm^3/kg d.a.f. fuel in Figure 10. This behavior is consistent with our general anticipation that high-temperature pyrolysis produces more noncondensable gases and fewer tars. Nonetheless, Figure 10 clarifies further that the increase in the pyrolysis gas yield at temperatures above 600°C might be mainly due to the increased yield in H_2.

The preceding results of biomass pyrolysis from the MFBRA are comparable to the data measured by Deglise et al.[13] in a free drop-tube reactor for dry-wood pyrolysis at a heating rate of 1000°C/s. This notwithstanding, certain differences existed with the report of Dufour et al.[14] on wood powder pyrolysis in a heated tube furnace in N_2 atmosphere. In their tests, the sample was introduced into the center of a preheated tube. They found that the volume of released H_2 gradually increased from 700 to 1000°C (0.06–0.24 Nm^3/kg d.a.f. biomass), whereas the CO production increased from 700 to 800°C (0.27–0.32 Nm^3/kg d.a.f. biomass) but remained in constant between 800 and 1000°C. Different heating rates in the MFBRA from that in the tube furnace adopted by Dufour et al. should be the cause for the differences in pyrolysis gas production. Concerning the consistency of our data with that of Deglise et al., we may believe that the realized heating rate in the MFBRA was much higher than that in the tube furnace.

Obviously, all the aforementioned new identifications regarding the pyrolysis in MFBRA would allow deep insights into the reaction mechanics of pyrolysis, showing another merit and big application of the instrument.

Pyrolysis of coal in MFBRA

Pyrolysis of coal was also tested in MFBRA at 500–900°C. Figures 11 and 12 show, respectively, the time-dependent gas release measured at 800°C and the temperature-dependent variations of the totally produced volumes for major gas components. The sequence characteristics of gas release demonstrated in Figure 11 was quite similar to that

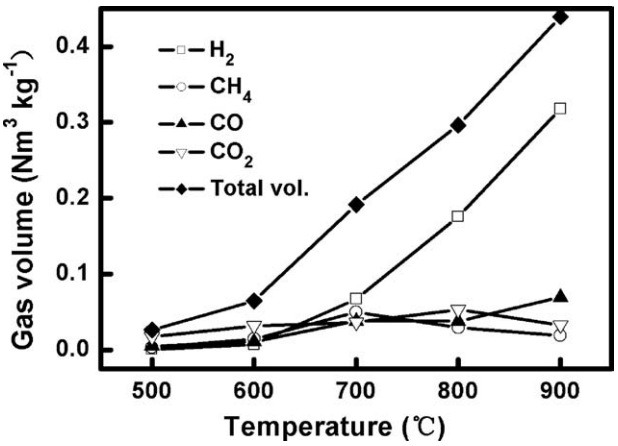

Figure 12. Permanent gas volume (Nm^3/kg a.d. coal) as a function of reaction temperature for coal pyrolysis.

in Figure 9. Although the produced gas started to release by following a sequence of CO_2, H_2, CO, and CH_4, the end of the gas release was subjected to CO_2, CH_4, CO, and H_2 in succession. The time span to evolve an individual gas was also longest for H_2 and comparable for CH_4 and CO, but the released CO_2 appeared greater and also in a longer span in comparison with that in Figure 9.

In comparison with biomass pyrolysis (Figure 10), Figure 12 demonstrates that the produced CO, CO_2, and CH_4 were less than the generated H_2. The generated CO, CO_2, and CH_4 also varied little with temperature over the temperature range of 500–900°C, and the absolute volumes were all about 0.055 Nm^3/kg d.a.f. coal and was evidently lower than those in Figure 10 for biomass. For CO_2 and CH_4, there existed peak productions at 700°C and 800°C, respectively. These temperatures are higher than the 600°C and 700°C for biomass in Figure 10. Although the H_2 production increased with raising temperature, the highest volume at 900°C was only 0.32 Nm^3/kg d.a.f. coal, lower than 0.43 Nm^3/kg d.a.f. biomass in Figure 10.

The above results demonstrate that the pyrolysis of biomass generated more noncondensable gases than coal pyrolysis, and the maximal production of individual gases occurred at higher temperatures for coal pyrolysis. These observations comply with the fact that biomass fuel contains more volatiles and has higher reactivity to pyrolyze. Furthermore, the results are in general agreement with the finding of Desypris et al.[15] who tested pyrolysis of a kind of 44 μm coal in a 15 mm i.d. fluidized bed reactor. This, thus, verified further that the developed MFBRA provided a reliable tool to analyze gas–solid reactions including pyrolysis.

Conclusions

To overcome shortcomings of thermogravimetric (TG) methods (e.g., not enabling sample feed at a specified temperature and suffering from interfacial diffusion limitations in TG cell), the so-called micro-fluidized bed reaction analyzer (MFBRA) was developed to be a standard reaction analysis tool for gas–solid reactions. The analyzer was applied to measure thermal decomposition of $CaCO_3$ powder, CuO reduction in CO, and pyrolysis of biomass and coal fuels in this study, demonstrating that the developed MFBRA provided good repeatability and reliability for measuring these gas–solid reactions. The derived apparent activation energy of $CaCO_3$ decomposition from MFBRA was obviously smaller than that from TG, clarifying that the MFBRA enabled quicker decomposition reaction. Obviously, quicker reaction was shown also with reduction of CuO in CO at a specified reaction temperature. The suppressed external diffusion and higher heating rate prevailing in MFBRA were responsible for all these demonstrated advantages of the MFBR.

Measurement of pyrolysis of coal and biomass in MFBRA identified a time of about 10 s to finish pyrolysis reactions, which is much closer to the theoretically expected time in comparison with the other literature reports from using fluidized beds of tens of millimeters in diameter. It demonstrated that the gases H_2, CO, CO_2, and CH_4 produced by the pyrolysis in MFBRA had different times to start and end their releases, and the generated gas volume had also different variation features with the reaction temperature for different gas species. Although the gases followed a sequence of CO_2, H_2, CO, and CH_4 to start release, the end of release was subjected to CO_2, CH_4, CO, and H_2 in succession. Of all these gas species, only H_2 gradually increased in its released amount with raising the temperature, and the amount of released CO_2 manifested the least variation with temperature. Peak production at a temperature between 600°C and 800°C was identified for both CH_4 and CO, but the critical temperature for the peak production was higher for coal. These findings from the MFBRA would enable a deep insight into the pyrolysis mechanics.

Acknowledgments

The authors are grateful to financial supports of Chinese Academy of Sciences (Y2005014) and National Natural Science Foundation of China (20606034, 20776144). Acknowledgments are also extended to Dr. Yin Wang, Dr. Xinhua Liu, and Ms. Mei Zhong for their helps on experiments.

Literature Cited

1. Rajic M, Suceska M. Study of thermal decomposition kinetics of low-temperature reaction of ammonium perchlorate by isothermal TG. *J Therm Anal Calorim*. 2001;63:375–386.
2. De Jong W, Pirone A, Wojtowicz MA. Pyrolysis of miscanthus giganteus and wood pellets: TG-FTIR analysis and reaction kinetics. *Fuel*. 2003;82:1139–1147.
3. Yakuphanoglu F, Yoo YT. Kinetics analysis of the thermal decomposition of poly(butylene adipate) ionomers by thermogravimetry (TG) and derivate (DTG) analysis. *J Macromol Sci Part A: Pure Appl Chem*. 2005;43:647–654.
4. Wang BB, Hu GS, Wei LX. Melting behavior, nonisothermal crystallization kinetics, and morphology of PP/nylon 11/EPDM-Tg-MAH blends. *J Appl Polym Sci*. 2008;107:3013–3022.
5. Liu JX, Xu HY. Study on the regeneration of deactivated NiO/γ-Al2O3 catalyst for the conversion of natural gas with CO2 to synthesis gas by TG. *Thermochim Acta*. 2000;343:99–104.
6. Sanders JP, Gallagher PK. Kinetics of the oxidation of magnetite using simultaneous TG/DSC. *J Therm Anal Calorim*. 2003;72:777–789.
7. Pap IS, Szepvolgyi J, Bertoti I, Mink G, Szekely T. TG study on the reduction kinetics of hematite and iron oxide-containing wastes. *J Therm Anal*. 1988;33:575–583.
8. Liu XH, Xu GW, Gao SQ. Micro fluidized beds: wall effect and operability. *Chem Eng J*. 2008;137:302–307.

9. Budrugeac P, Segal E. Some methodological problems concerning nonisothermal kinetic analysis of heterogeneous solid-gas reactions. *Int J Chem Kinet*. 2001;33:564–573.
10. Asaki Z, Fukunaka Y, Nagase T, Kondo Y. Thermal decomposition of limestone in a fluidized bed. *Met Trans*. 1974;5:381–390.
11. Vyazovkin S, Wight CA. Kinetics in solids. *Annu Rev phys Chem*. 1997;48:125–149.
12. Xu GW, Murakami T, Suda T, Matsuzawa Y, Tani H. Dual fluidized bed gasification of coffee grounds: performance evaluation and parameter influence. *Energy Fuels*. 2006;20:2695–2627.
13. Deglise X, Richard C, Rolin A, Francois H. Effects of temperature and humidity on flash pyrolysis of lignocellulosic wastes. *Rev Gen Therm*. 1980;227:871–880.
14. Dufour A, Girods P, Masson E, Rogaume Y, Zoulalian A. Synthesis gas production by biomass pyrolysis: effect of reactor temperature on product distribution. *Int J Hydrogen Energy*. 2009;34:1726–1734.
15. Desypris J, Murdoch P, Williams A. Investigation of the flash pyrolysis of some coals. *Fuel*. 1982;61:807–816.

Manuscript received Jun. 1, 2009, revision received Dec. 21, 2009, and final revision received Feb. 4, 2009.